Mach shock waves and surface effects in metals

1995 J. Phys.: Condens. Matter 7 9465

(http://iopscience.iop.org/0953-8984/7/49/011)

J. Phys.: Condens. Matter 7 (1995) 9465–9473. Printed in the UK

Mach shock waves and surface effects in metals

K Griepenkerl, A Schäfer and W Greiner

Institut für Theoretische Physik, Johann Wolfgang Goethe-Universität, Frankfurt am Main, Germany

Received 20 September 1995

Abstract. We calculate the electric potential induced by a fast ion in a conducting solid close to its surface. The ion velocity is supposed to exceed the Fermi velocity in the metal; thus Mach shock waves are induced. Calculations are done within an electron gas approximation; the surface effects are described according to the 'specular reflection model'.

1. Introduction

When a fast projectile emerges from a solid target, electrons are emitted from its surface. A small fraction of these electrons are emitted by the shock wave associated with the ion. If the projectile velocity exceeds the Fermi velocity of the solid, the angle between the emitted shock electrons and the ion is determined by the Mach angle in the solid [1, 2]. In a first approximation, these electrons are emitted perpendicular to the front of the Mach shock cone. The emission of such electrons was confirmed experimentally [3]. The detailed experimental investigation and theoretical analyses of their properties looks promising as regards study of the dielectric properties of solids and their surface properties. The theoretical description requires two steps. First the electron-transport properties in an idealized solid including the surface effects have to be calculated. In a second step, specific, phenomenological corrections will have to be introduced to describe additional effects of a realistic surface. This second part is not dealt with in this contribution. For example it was observed experimentally that even a very thin layer of light atoms changes the properties of the emitted electrons. In this contribution we deal with the first part of the problem, namely the idealized case of a perfect surface.

The canonical approach for a consideration of surface effects starts by finding an appropriate dielectric function ε. This function has the form $\varepsilon(\boldsymbol{r}, \boldsymbol{r}', t)$ and can only be given implicitly in the form of integral equations which makes the further analyses of dynamical properties very cumbersome. Thus, this approach is not feasible for practical calculations. Instead, we choose the specular reflection model [4], in which the electrodynamic properties close to the surface are approximated by the bulk dielectric function with appropriate boundary conditions.

We assume the surface between the medium and the vacuum to be at $z = 0$. The vacuum is chosen to lie to the left ($z < 0$) and the medium to the right; see figure 1.

A full electrodynamic description of this problem can theoretically be given once the dielectric function ε is known. In the specular reflection model all effects of the surface are absorbed into the definition of a surface charge σ such that the remaining dielectric function is that of an infinite homogeneous solid $\varepsilon = \varepsilon(r, r', t, t') \to \varepsilon(r - r', t - t')$. The

0953-8984/95/499465+09$19.50

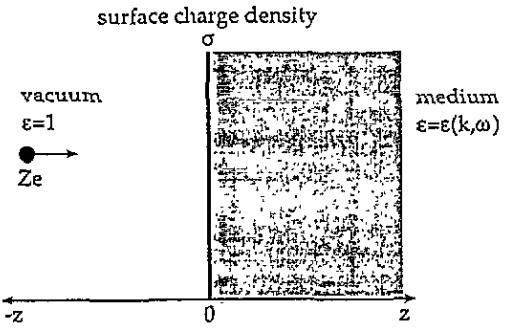

Figure 1. The problem under consideration: the projectile moves from left to right, the surface is located at $z = 0$.

procedure is analogous to the introduction of mirror charges in classical electrostatics. In this framework the potential ϕ_{ind} and the electron density η_{ind} induced in the medium can be calculated as functions of $\tilde{\rho}(K, \omega)$, which in turn are defined by the boundary conditions for the electric potential and the dielectric displacement at the surface (see equations (9) and (10)).

For comparison and illustration we start by discussing the homogeneous case (without a surface) and discuss afterwards the necessary modifications for including the boundary. In the homogeneous case the equations for η_{ind} and ϕ_{ind} read

$$\begin{aligned}\eta_{\text{ind}}(\bar{z}, \rho) &= \frac{Ze}{(2\pi)^2}\int_0^\infty \mathrm{d}K\, K J_0(K\rho)\int_{-\infty}^{+\infty}\mathrm{d}\omega\, \frac{\mathrm{e}^{\mathrm{i}(\omega/v)\bar{z}}}{\tilde{\varepsilon}(k,\omega)}\\ \phi_{\text{ind}}(\bar{z}, \rho) &= \frac{Ze}{(2\pi)^2}\int_0^\infty \mathrm{d}K\, K J_0(K\rho)\int_{-\infty}^{+\infty}\mathrm{d}\omega\, \frac{\mathrm{e}^{\mathrm{i}(\omega/v)\bar{z}}}{k^2\tilde{\varepsilon}(k,\omega)}\end{aligned} \tag{1}$$

where the projectile trajectory is taken to be $z = vt + \bar{z}, x = 0, y = 0$ with $\bar{z}$ being the z-coordinate in the projectile rest system and $K = \sqrt{k^2 - k_z^2}$ being the transverse momentum. The tilde signifies the Fourier transform, which we use in the form

$$\tilde{f}(k) = \frac{1}{\sqrt{2\pi}}\int_{-\infty}^{+\infty}\mathrm{d}x\ \mathrm{e}^{-\mathrm{i}kx} f(x). \tag{2}$$

In this paper we will use the hydrodynamic dielectric function

$$\tilde{\varepsilon}(k,\omega) = 1 + \frac{\omega_p^2}{u^2k^2 - (\omega - \mathrm{i}\delta)^2} \qquad \text{with } u^2 = \frac{3}{5}v_F^2 \tag{3}$$

where v_F is the Fermi velocity and ω_p the plasma frequency which is treated as an empirical parameter.

The electric potential and the electron density in the bulk solid calculated with this ε are shown in figures 2 and 3. The density clearly shows the Mach cone. For the potential, the wakes are nearly perpendicular to the ion trajectory and a cone structure can only faintly be discerned.

2. The treatment of surface effects

In order to describe the surface, a surface charge σ is introduced such that $\theta(\boldsymbol{r}, t) = \sigma(x, y, t)\,\delta(z)$ and

$$\tilde{\sigma}(\boldsymbol{K}, \omega) = \int \mathrm{d}\boldsymbol{R}\,\mathrm{d}t\ \mathrm{e}^{-\mathrm{i}(\boldsymbol{K}\cdot\boldsymbol{R} - \omega t)}\sigma(x, y, t). \tag{4}$$

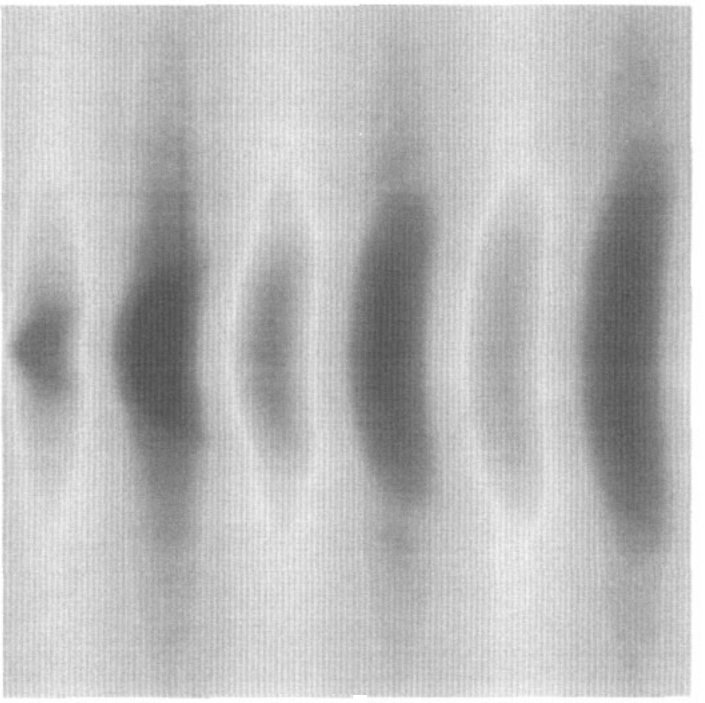

Figure 2. The potential induced in a solid by a projectile. U on Al at $E_{\text{ion}} = 0.93$ MeV u^{-1}.

This surface charge induces the potential

$$\tilde{\phi}^{\text{Med}}(\boldsymbol{K}, z, \omega) = \frac{\tilde{\sigma}(\boldsymbol{K}, \omega)}{\sqrt{2\pi}\varepsilon_0} \int_{-\infty}^{+\infty} \mathrm{d}k_z \, \mathrm{e}^{\mathrm{i}k_z z} \frac{1}{\tilde{\varepsilon}(\boldsymbol{k}, \omega)k^2}. \tag{5}$$

To proceed we shall treat the two cases separately starting with the first one:

(i) projectile in the vacuum ($t < 0$), potential in the solid ($z > 0$);
(ii) projectile in the solid ($t > 0$), potential in the solid ($z > 0$).

In the absence of any charge the potential in the vacuum decays exponentially with increasing distance from the surface (far from a neutral solid there is no potential). The Poisson equation in the left half-space without the external charge (the projectile) and its solution read

$$\left(\partial_z^2 - K^2\right)\tilde{\phi}^{\text{Vac}}(\boldsymbol{K}, z, \omega) = 0 \qquad \tilde{\phi}^{\text{Vac}}(\boldsymbol{K}, z, \omega) = A(K, \omega)\mathrm{e}^{Kz} \tag{6}$$

where the boundary condition $\lim_{z\to-\infty}\phi_{\text{Vac}}(z) = 0$ was chosen (note that Kz is negative).

When the projectile is in the vacuum its charge density $\eta_{\text{ex}} = Ze\,\delta(\boldsymbol{r} - \boldsymbol{v}t)$ induces the potential

$$\tilde{\phi}^{\text{ex}}(\boldsymbol{K}, z, \omega) = \frac{Zev}{(2\pi)^{3/2}\varepsilon_0} \frac{\mathrm{e}^{\mathrm{i}(\omega/v)z}}{K^2v^2 + \omega^2}. \tag{7}$$

in the vacuum. Thus the complete solution for the potential in the left half-space reads

$$\tilde{\phi}^{\text{Vac}}(\boldsymbol{K}, z, \omega) = \frac{Zev}{(2\pi)^{3/2}\varepsilon_0} \frac{\mathrm{e}^{\mathrm{i}(\omega/v)z}}{K^2v^2 + \omega^2} + A(K, \omega)\mathrm{e}^{Kz}. \tag{8}$$

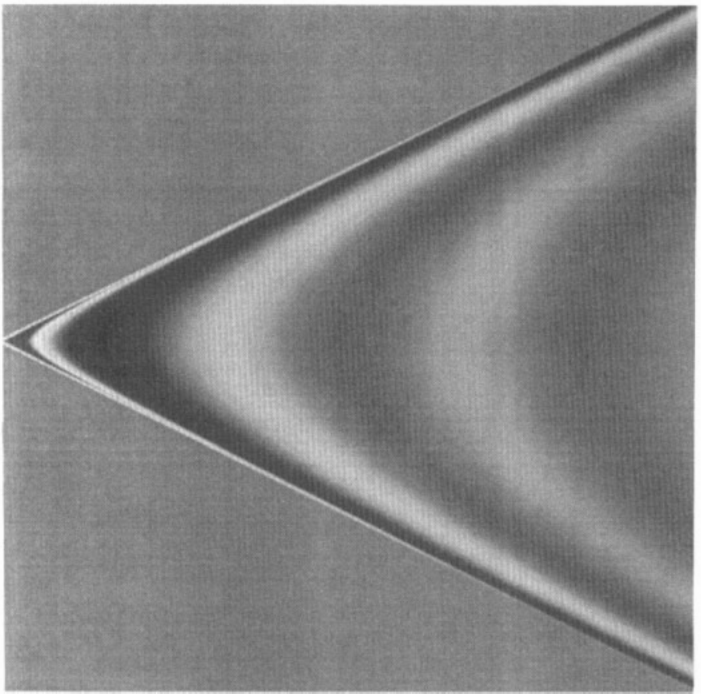

Figure 3. The charge density corresponding to figure 2. U on Al at $E_{\text{ion}} = 0.93$ **MeV u**$^{-1}$.

In order to determine the two parameters $A(K,\omega)$ and $\sigma(K,\omega)$ we require at the boundary $z = 0$, i.e.

$$\frac{\tilde{\sigma}(K,\omega)}{\sqrt{2\pi}\varepsilon_0}\int_{-\infty}^{+\infty}\frac{\mathrm{d}k_z}{\tilde{\varepsilon}(k,\omega)k^2} = \frac{Zev}{(2\pi)^{3/2}(K^2v^2+\omega^2)\varepsilon_0} + A \tag{9}$$

$$\frac{\tilde{\sigma}(K,\omega)}{2} = -\frac{\mathrm{i}Ze\omega}{(2\pi)^{3/2}(K^2v^2+\omega^2)} - \varepsilon_0 AK. \tag{10}$$

We make use of the cylindrical symmetry of the problem and of the relation [5]

$$\int_0^{2\pi}\mathrm{d}\phi_k\ \mathrm{e}^{\pm\mathrm{i}k_r r_\perp\cos\phi_k} = 2\pi J_0(k_r r_\perp)$$

to simplify equations (5) and (8):

$$\phi_{\text{ind}}(\rho,z,t) = \phi^{\text{Vac}}(\rho,z,t) + \phi^{\text{Med}}(r,t)$$

$$\phi^{\text{Vac}}(\rho,z,t) = \frac{Ze}{(2\pi)^{5/2}\varepsilon_0}\int \mathrm{d}K\ K\ \mathrm{d}\omega\ J_0(K\rho)\frac{\mathrm{e}^{-\mathrm{i}\omega t+Kz}}{\omega^2+K^2v^2}\frac{\mathrm{i}\,2\sqrt{2\pi}\omega I_0 - 2\pi v}{\sqrt{2\pi}-2KI_0}$$

$$\phi^{\text{Med}}(r,t) = \frac{1}{(2\pi)^2\varepsilon_0}\int \mathrm{d}K\ K\ J_0(KR)\int \mathrm{d}\omega\ \mathrm{e}^{\mathrm{i}\omega t}\tilde{\sigma}(K,\omega)I_z(K,\omega) \tag{11}$$

where

$$I_z(K,\omega) = \int_{-\infty}^{+\infty}\mathrm{d}k_z\ \frac{\mathrm{e}^{\mathrm{i}k_z z}}{k^2\tilde{\varepsilon}(k,\omega)} \qquad I_0(K,\omega) = \lim_{z\to 0^+}\int_{-\infty}^{+\infty}\mathrm{d}k_z\ \frac{\mathrm{e}^{\mathrm{i}k_z z}}{k^2\tilde{\varepsilon}(k,\omega)}. \tag{12}$$

In the momentum integrals (11) and (12) an upper cut-off should be introduced for the following physical reason. At large momentum the treatment of the medium as a continuum is invalid as individual single-particle excitations become important. Therefore

all momentum integrals should be cut off at a critical value k_c. The results should be rather independent of the precise cut-off used, as is indeed the case; see figure 4. We find in fact that letting the cut-off go to infinity affects our results only marginally, except for in a case discussed below. Our results are also insensitive to the ratio of the cut-offs for k_z and K. To simplify our calculations we therefore take the opportunity of letting the k_z cut-off go to infinity, which allows us to calculate $I_z(K,\omega)$ analytically.

It turns out that the ω-integration cannot be done simply by calculating the residues for a suitable contour because $I_z(K,\omega)$ and $I_0(K,\omega)$ have cuts on the real axes and a discontinuity on the imaginary axes, proportional to $\Theta(Rk_z)$. The integration was therefore done by determining numerically the principal values. For the k_z-integration this implies that only real ω have to be considered as parameters. Under these circumstances, four cases have to be treated separately:

(1) $\omega^2 > \omega_p^2 + u^2K^2$, $\omega > 0$;
(2) $\omega^2 > \omega_p^2 + u^2K^2$, $\omega < 0$;
(3) $\omega^2 < \omega_p^2 + u^2K^2$, $\omega > 0$;
(4) $\omega^2 < \omega_p^2 + u^2K^2$, $\omega < 0$.

The resulting potential is $\phi^{\mathrm{Med}} = \phi_1^{\mathrm{Med}} + \phi_2^{\mathrm{Med}}$, where

$$\phi_1^{\mathrm{Med}}(R,z,t) = \frac{-Ze}{(2\pi)^{5/2}\varepsilon_0}\int \mathrm{d}K\ J_0(KR)\int_{|\omega|>\sqrt{\omega_p^2+u^2K^2}} \mathrm{d}\omega\ \mathrm{e}^{\mathrm{i}\omega t} \times \frac{\mathrm{e}^{-Kz}sw + \mathrm{i}\mathrm{e}^{-\mathrm{i}\chi wz/u}\omega_p^2 uK\chi}{(\mathrm{i}\omega + Kv)\left[w\left\{-(1+\sqrt{2\pi})s + \omega_p^2\right\} - \chi\mathrm{i}\sqrt{2\pi}\omega_p^2 uK\right]}$$

$$\phi_2^{\mathrm{Med}}(R,z,t) = \frac{-Ze}{(2\pi)^{5/2}\varepsilon_0}\int \mathrm{d}K\ J_0(KR)\int_{|\omega|<\sqrt{\omega_p^2+u^2K^2}} \mathrm{d}\omega\ \mathrm{e}^{\mathrm{i}\omega t} \times \frac{\mathrm{e}^{-Kz}sw - \mathrm{e}^{-wz/u}\omega_p^2 uK}{(\mathrm{i}\omega + Kv)\left[w\left\{-(1+\sqrt{2\pi}s + \omega_p^2\right\} + \sqrt{2\pi}\omega_p^2 uK\right]} \tag{13}$$

This double integral is solved numerically, where for the ω-integration the principal value is treated according to

$$\int_{\omega_j-\delta}^{\omega_j+\delta} \mathrm{d}\omega\ \frac{f(\omega)}{\omega-\omega_j} \approx 2\delta f'(\omega_j). \tag{14}$$

The derivatives f' were computed analytically with the help of *Mathematica* [6]. Only the roots of ω without imaginary parts are considered. As these roots ω_i are functions of K, it happens that two of these functions intersect for some $K \in [0, k_c]$. At this point, two poles of first order in ω give one pole of second order; thus the ω-integration, even in the principal-value interpretation, no longer makes sense. Looking at the two real functions $\omega_i(K)$, it is evident that one of the poles is the plasmon mode ω_p of the solid. The intersection is due to the fact that an interaction between different modes of the solid is not accounted for in the choice of the dielectric function. The physical interaction between these two collective modes will avoid the double pole due to the Landau–Zener effect, but this interaction is not included in our model. As calculations show that the potential only varies slightly with a variation of the upper integration limit in the region $[0.6k_c, 0.7k_c]$, we conclude that the contributions to the potential mainly come from the region $K \in [0, 0.7k_c]$, so we limit the integration to this region thus avoiding the troublesome double pole. We assume that the error introduced by this *ad hoc* procedure is relatively small. For small K

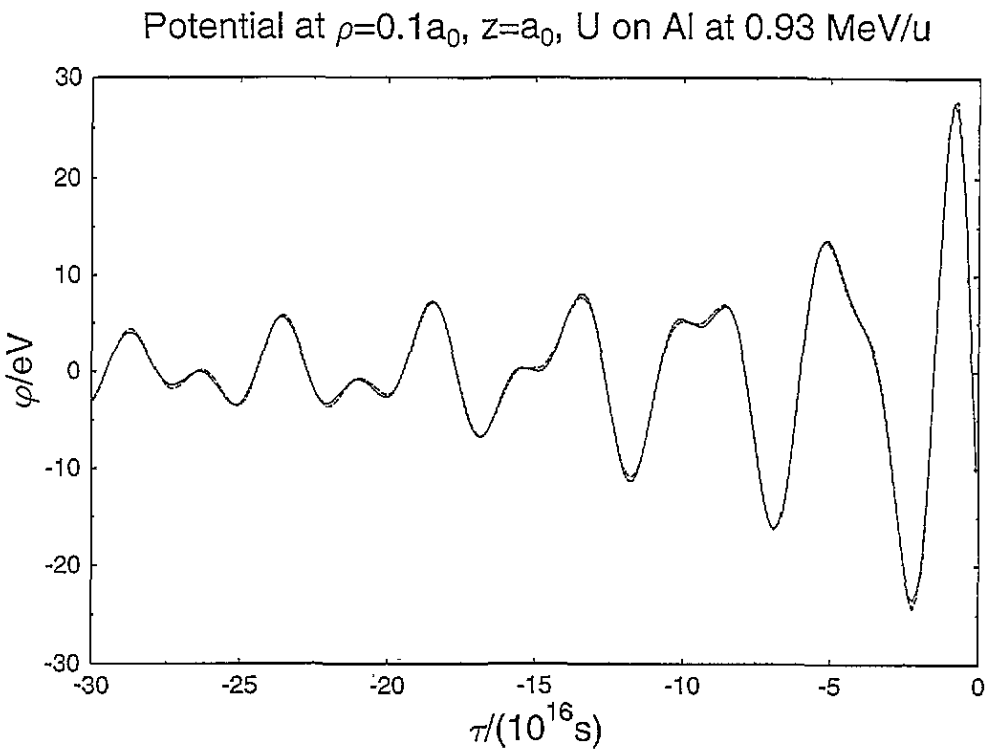

Figure 4. The time dependence of the potential at $z = 0$. The two curves differ by 10% in cut-off parameter.

one of the poles disappears, so there is no problem. The resulting potential for an aluminium target, a uranium ion, and the kinetic energy 0.93 MeV u^{-1} is shown in figure 5. The time dependence of the potential at $z = 0$ is shown for different K-integration boundaries in figure 4. The latter figure demonstrates the insignificance of the precise value chosen for k_c.

If the projectile is in the solid the treatment is completely analogous. The potential in the solid is given by

$$\tilde{\phi}(k,\omega) = \frac{\tilde{\rho}(k,\omega)}{k^2\tilde{\varepsilon}(k,\omega)\varepsilon_0}. \tag{15}$$

In order to fulfil the requirements of the specular reflection, a mirror charge $Ze\,\delta(z-vt)$ is introduced [4]. Thus, the effective charge is

$$\rho(r,t) = Ze\,\delta(x)\,\delta(y)\,\{\delta(z-vt)+\delta(z+vt)\}+\delta(z)\,\sigma(x,y,t) \tag{16}$$

and the Fourier transform yields

$$\tilde{\rho}(K,z,\omega) = \frac{Ze}{(2\pi)^{3/2}v}\cos\left(\frac{\omega}{v}z\right)+\delta(z)\,\tilde{\sigma}(K,\omega). \tag{17}$$

The contribution of the surface charge to the potential is given by

$$\varepsilon * \left(\Delta\phi^{\mathrm{Sur}}\right) = -\frac{1}{\varepsilon_0}\,\delta(z)\,\sigma(x,y,t) \tag{18}$$

where $*$ stands for a convolution. Thus,

$$\tilde{\phi}^{\mathrm{Sur}}(K,z,\omega) = \frac{1}{2\pi\varepsilon_0}\int \mathrm{d}k_z\ \mathrm{e}^{\mathrm{i}k_z z}\frac{\tilde{\sigma}(K,\omega)}{\tilde{\varepsilon}k^2} \tag{19}$$

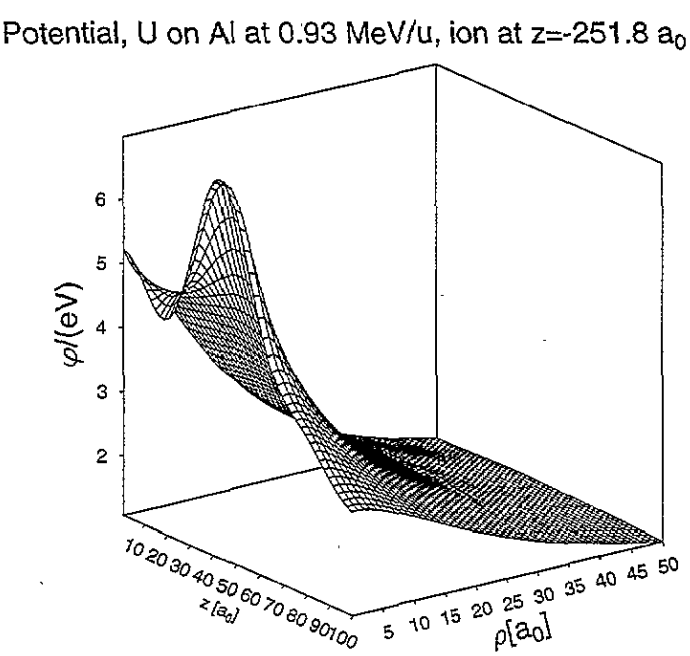

Figure 5. A three-dimensional representation of the potential; the projectile is in the vacuum at $z = -251.8\ a_0$.

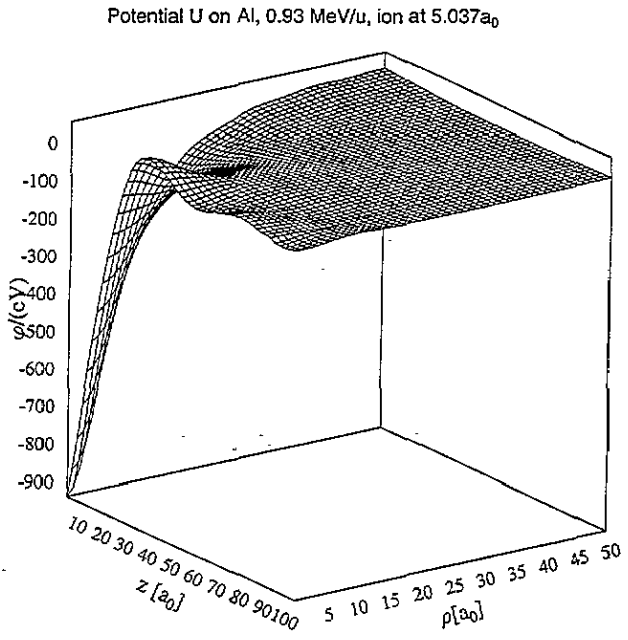

Figure 6. A three-dimensional representation of the potential; the projectile is in the target at $z = 5.037\ a_0$.

and the effective potential is

$$\tilde{\phi}^{\mathrm{Med}}(\boldsymbol{K}, z, \omega) = \frac{Ze}{(2\pi)^{3/2} v \varepsilon_0} \int \mathrm{d}k_z \, \frac{\mathrm{e}^{\mathrm{i}k_z z}}{k^2 \tilde{\varepsilon}(\boldsymbol{k}, \omega)} \cos\left(\frac{\omega}{v} z\right) + \frac{\tilde{\sigma}(\boldsymbol{K}, \omega)}{2\pi \varepsilon_0} \int \mathrm{d}k_z \, \frac{\mathrm{e}^{\mathrm{i}k_z z}}{\tilde{\varepsilon} k^2}. \tag{20}$$

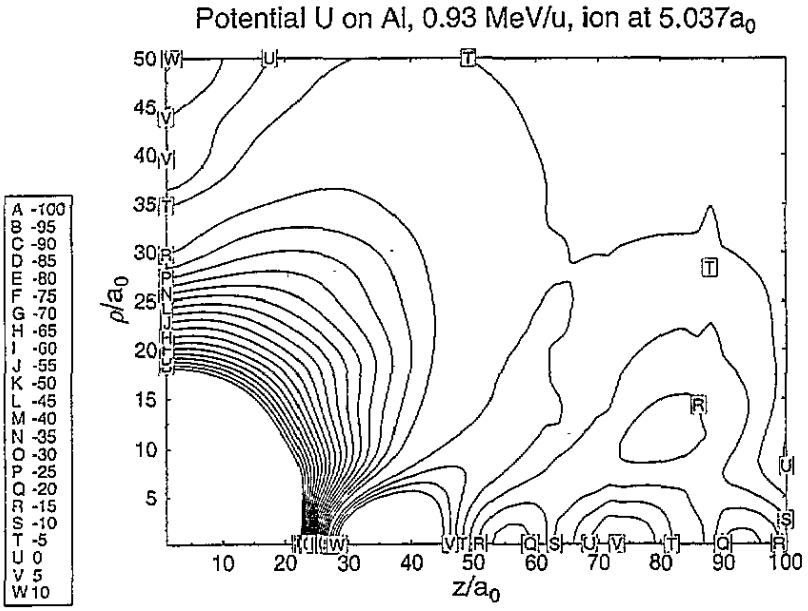

Figure 7. A contour plot of the potential from figure 6.

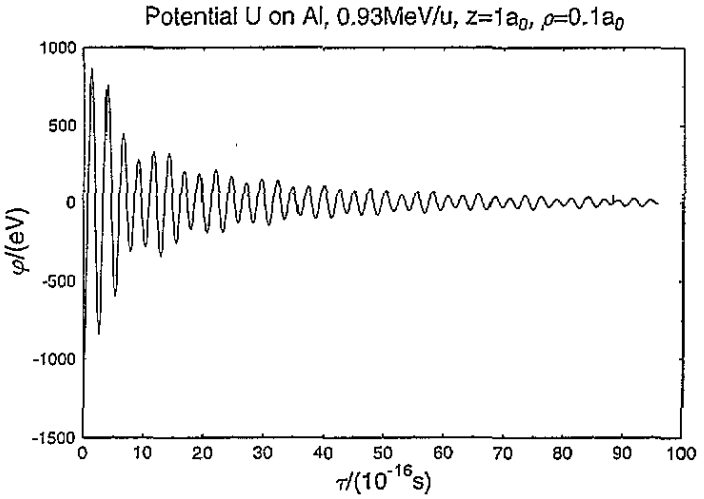

Figure 8. The time dependence of the potential at $z = 0$. The projectile starts at $z = 5.037\ a_0$ for $t = 0$.

For the potential in the vacuum we insert again $\tilde{\phi}^{\mathrm{Vac}} = Ae^{Kz}$. The two parameters $A(K, \omega)$ and $\tilde{\sigma}(K, \omega)$ are again determined by the requirement of continuity of ϕ and D at $z = 0$. The procedure in this case is straightforward and follows the lines of the case of the projectile in the vacuum—only, in this case, there is no double pole for $0 \leqslant K \leqslant k_c$.

The potential is shown for a specific target and ion in figures 6 and 7. In addition, the time dependence of the potential at $z = 0$ is shown in figure 8.

3. Conclusions

We have developed a model which allows us to calculate the dynamical potentials and electron densities in a solid and outside of it, during the passage of a fast ion. From our time-dependent electron densities we can already calculate the corresponding electron currents. However, these cannot yet be compared with the observed emitted electrons as we still have to include corrections due to the less than perfect properties of realistic surfaces, which will be the topic of future investigations.

Acknowledgments

We are very grateful to K-O Groeneveld and his group for helpful discussions. This work was supported by DFG and BMFT.

References

[1] Schäfer W, Stöcker H and Greiner W 1980 Mach-shock electron distributions from solids *Z. Phys.* B **36** 319–22

[2] Schäfer W, Stöcker H and Greiner W 1978 Mach cones induced by fast heavy ions in electron plasma *Z. Phys.* A **288** 349–52

[3] Rothard H, Burkhard M, Kemmler J, Biedermann C, Kroneberger K, Koschar P, Heil O and Groeneveld K O 1988 Shock electrons from ion–solid penetration *J. Physique Coll.* **48** C9 211

[4] Ritchie R H and Marusak A L 1966 The surface plasmon dispersion relation for an electron gas *Surf. Sci.* **4** 231–40

[5] Abramowitz M and Stegun I A (ed) 1965 *Handbook of Mathematical Functions* (New York: Dover)

[6] Wolfram S 1991 *Mathematica. A System for Doing Mathematics by Computer* 2nd edn (Redwood City, CA: Addison-Wesley)